Misdiagnosis of chordoma: A case report and a review of the literature

DONG LI[1], MENGMENG ZHANG[1], PING ZHANG[2], TAO WANG[3] and CHEN JIANG[1]

[1]Department of Pathology, Qingdao Municipal Hospital, Qingdao, Shandong 266000, P.R. China;
[2]Department of Gynecology, Qingdao Municipal Hospital, Qingdao, Shandong 266000, P.R. China;
[3]Department of Radiology, Qingdao Municipal Hospital, Qingdao, Shandong 266000, P.R. China

Received October 22, 2024; Accepted February 21, 2025

DOI: 10.3892/ol.2025.15057

Abstract. The present study aimed to investigate the clinicopathological features and diagnostic criteria for differentiating between chordoma and chordoid meningioma. A case of chordoma was retrospectively analyzed using clinical, radiographic, histological and immunohistochemical data, alongside a literature review. A 59-year-old male patient was admitted with headaches and dizziness persisting for 2 months without any obvious precipitating factors. The patient underwent two intracranial tumor resections between March 2022 and December 2023. The pathology report from the first surgery indicated that the tumor was composed of cords of epithelioid cells with vacuolated cytoplasm embedded in a basophilic stroma. Immunohistochemical analysis showed positivity for cytokeratin, vimentin, epithelial membrane antigen, synaptophysin, cytokeratin 8/18 and E-cadherin, with a Ki-67 proliferation index of 3%. Progesterone receptor, D2-40, glial fibrillary acidic protein, S100 and SOX10 staining were negative. Based on the pathology and immunohistochemical findings, the diagnosis was determined to be a chordoma-like meningioma (World Health Organization Grade 2). The pathology report from the second surgery revealed a tumor composed of cords and isolated epithelioid cells with intracytoplasmic vacuoles within a myxoid matrix. However, immunohistochemical analysis indicated positivity for Brachyury, leading to a diagnosis of chordoma. In conclusion, the histological morphology of chordoma is similar to that of chordoid meningioma and lacks clinical specificity. Immunohistochemical staining of tumor markers assists in both the diagnosis and differential diagnosis. Currently, treatment for chordoma and choroid mengioma primarily focuses on surgical resection, which is associated with high rates of relapse. The differential diagnosis predominantly influences the postoperative treatment strategy.

Introduction

Chordoma is a rare primary malignant bone tumor that originates from the embryonic remnants of the notochord. Chordoma typically arises in the skull base or sacrum, with an annual incidence rate of ~0.8 cases per million individuals, accounting for ~1% of all bone tumors (1). Chordomas can manifest at any age, but the majority of patients are diagnosed between the ages of 40 and 50 years. Clinical manifestations primarily depend on the location and extent of the lesions, with intracranial chordomas often causing headaches or facial numbness due to their proximity to cranial nerves, while sacrococcygeal chordomas may lead to lumbosacral pain or bowel dysfunction due to compression of the sacral nerve roots (1).

Chordoid meningioma, on the other hand, is a rare subtype of meningioma, accounting for 0.5-1% of all meningiomas (2). This tumor is more commonly found in young female patients and is typically located in the supratentorial region or at the skull base (3). Chordoid meningiomas can invade surrounding tissues, leading to symptoms such as headaches, vomiting and visual disturbances (2,3).

Given the overlapping clinical and pathological features of chordoma and chordoid meningioma, accurate differentiation between these two entities is crucial for appropriate treatment and prognosis. Misdiagnosis can lead to inappropriate therapeutic strategies, potentially affecting patient outcomes (4). The present case report aims to highlight the challenges in differentiating between chordoma and chordoid meningioma, emphasizing the importance of immunohistochemical markers and imaging studies in achieving an accurate diagnosis.

Case report

In March 2022, a 59-year-old male patient presented to the Qingdao Municipal Hospital (Qingdao, China) with a 2-month headache, dizziness and numbness in the right hand. The symptoms intensified when the patient lowered their head and rolled their neck. Notably, the severity of these symptoms

Correspondence to: Dr Chen Jiang, Department of Pathology, Qingdao Municipal Hospital, 1 Jiaozhou Road, Qingdao, Shandong 266000, P.R. China
E-mail: 1744392098@qq.com

Abbreviations: MRI, magnetic resonance imaging; PFS, progression-free survival; OS, overall survival

Key words: chordoma, chordoid meningioma, misdiagnosis, pathology, imaging

had increased over the past month. The physical examination revealed normal limb movements, gait and consciousness, as well as clear speech. The bilateral pupils were equal in size and shape, and exhibited a light reaction, and the patient displayed symmetrical forehead lines and nasolabial grooves on both sides. Tongue extension was centered. Muscle strength in the limbs was rated at level 5, muscle tone was normal (5) and blood pressure readings were within the normal range. The patient had no abnormal results in routine laboratory tests. Magnetic resonance imaging (MRI) revealed a round lesion in the left cerebellar hemisphere, characterized by long T1 and long T2 signals, with T2-weighted-fluid-attenuated inversion recovery exhibiting high signal intensity and unevenness. The lesion measured ~39 mm in diameter, had clear boundaries and was located adjacent to the lateral margin of the cerebellum, with diffusion-weighted imaging (DWI) showing an iso-low signal. MRI enhancement demonstrated moderate, uneven enhancement of the left cerebellar hemisphere lesion, featuring a central non-enhanced area and mild enhancement of the surrounding wall. The MRI findings were indicative of a 'space-occupying lesion in the left cerebellar hemisphere' (Fig. 1A). There was no prior history of tumors. The patient underwent an intracranial tumor resection in March 2022. Following the procedure, the vital signs and overall condition of the patient were stable. Subsequently, the planning target volume (PTV) for radiotherapy following the first operation was 5,040 cGy/180 cGy/28 fractions, and mannitol injection (20%) in a volume of 150 ml once was provided to reduce intracranial pressure.

The gross resected specimen was formed of grey-white-brown broken tissue, with a total size of 2.5x2x2 cm, and the local tissue section was soft and spongy. Postoperative pathology (Data S1) revealed that the tumor was composed of cords of epithelioid cells with vacuolated cytoplasm and collagen fibers within a basophilic stroma (Fig. 2A and B). Immunohistochemical analysis (Data S1) revealed positivity for cytokeratin (CK), cytokeratin 8/18 (CK8/18), vimentin, epithelial membrane antigen (EMA), synaptophysin and E-cadherin, with a Ki-67 proliferation index of 3% (Fig. 3A-G). The tumor was negative for S100, glial fibrillary acidic protein (GFAP), progesterone receptor (PR), D2-40 and SOX-10 (data not shown). Based on the pathological and immunohistochemical findings, a diagnosis of chordoma-like meningioma [World Health Organization (WHO) Grade 2] (6) was made.

In November 2023, the patient experienced numbness on the right side of the face, without accompanying symptoms of headaches or dizziness. Neurological examination revealed no abnormalities. An MRI revealed irregular mass enhancement in the left Sylvian fissure cistern, with a cross-sectional area of ~22x18 mm, suggestive of an intracranial occupying lesion (Fig. 1B). In November 2023, the patient underwent another intracranial tumor resection. Postoperatively, the condition of the patient remained stable. The patient received radiotherapy for intracranial lesions and the lumbosacral area in December 2023. The PTV for radiotherapy after the second operation was 4,000 cGy/200 cGy/20 fractions for the intracranial lesion and 7,000 cGy/200 cGy/35 fractions for the lumbosacral lesion. At 1 month after the completion of radiotherapy, the efficacy evaluation indicated a partial response.

The gross specimen of the second surgery consisted of grey and broken tissue, with a diameter of 0.3 cm. The pathology results revealed that the tumor was composed of cords and isolated epithelioid cells, which exhibited intracytoplasmic vacuoles within a myxoid matrix (Fig. 2C and D). Immunohistochemical analysis revealed positive CK (Fig. 3H), Brachyury (Fig. 3I) and weakly-positive S100 (Fig. 3J) expression. These immunohistochemical findings suggested a diagnosis of chordoma.

A review of the hematoxylin and eosin slices from the first surgery in 2022 indicated that the epithelioid cells were arranged in a cord-like distribution within an eosinophilic mucinous matrix. Some cells exhibited eosinophilic cytoplasm, while others appeared vacuolated. Classic meningioma structures were absent, and there was no evidence of lymphocyte or plasma cell infiltration at the tumor periphery in a layered pattern. Repeat immunohistochemistry confirmed that the original slices were Brachyury-positive (Fig. 3K), further supporting the diagnosis of chordoma.

Postoperative follow-up in March 2024 revealed a patchy, low-density area in the left cerebellar surgical site, measuring ~24.7x19.4 mm. Additionally, soft-tissue nodules on the periphery and below, with a cross-section of ~25.6x15.0 mm, fluorodeoxyglucose hypermetabolic lesions in the peripheral and inferior regions of the left cerebellar surgical site and multiple hypermetabolic lymph nodes in the bilateral neck were noted on positron emission tomography-computed tomography (PET-CT) (Fig. 1C-E). Given the possibility of tumor recurrence and metastasis, palliative radiotherapy at 6,000 cGy/200 cGy/30 fractions was administered to the affected area. The efficacy evaluation indicated progressive disease 1 month after the completion of radiotherapy. In September 2024, the patient came to the hospital for re-examination due to dizziness and constipation. MR enhanced scanning examination showed the formation of softening lesions in the left cerebellar hemisphere and abnormal enhancement in the left insular-Sylvian cistern area (Fig. 1F). Follow-ups were organized and the patient was advised to return if symptoms worsened.

In November 2024, the patient presented to the hospital with paroxysmal headaches and dizziness. An enhanced MRI of the lumbosacral spine revealed nodular abnormal signal foci in the sacral canal at the S1-2 level, indicating a chordoma (Fig. 1G). Due to the progression of the disease in the brain, cranial radiotherapy was deemed inappropriate. Although the patient was advised to undergo comprehensive genetic testing, followed by targeted therapy and immunotherapy, the patient declined all these recommendations. The patient received a low dose of imatinib mesylate tablets (0.4 g, once daily) as targeted therapy, which resulted in slight alleviation of the dizziness (Table I). The patient sought treatment in Beijing following this visit and did not return to the hospital for a follow-up until February 2025, with the primary complaint still being dizziness. The clinician prescribed imatinib mesylate tablets (0.4 g, once daily) as a treatment.

Discussion

Chordoma is a rare primary malignant bone tumor that originates from the embryonic remnants of the notochord.

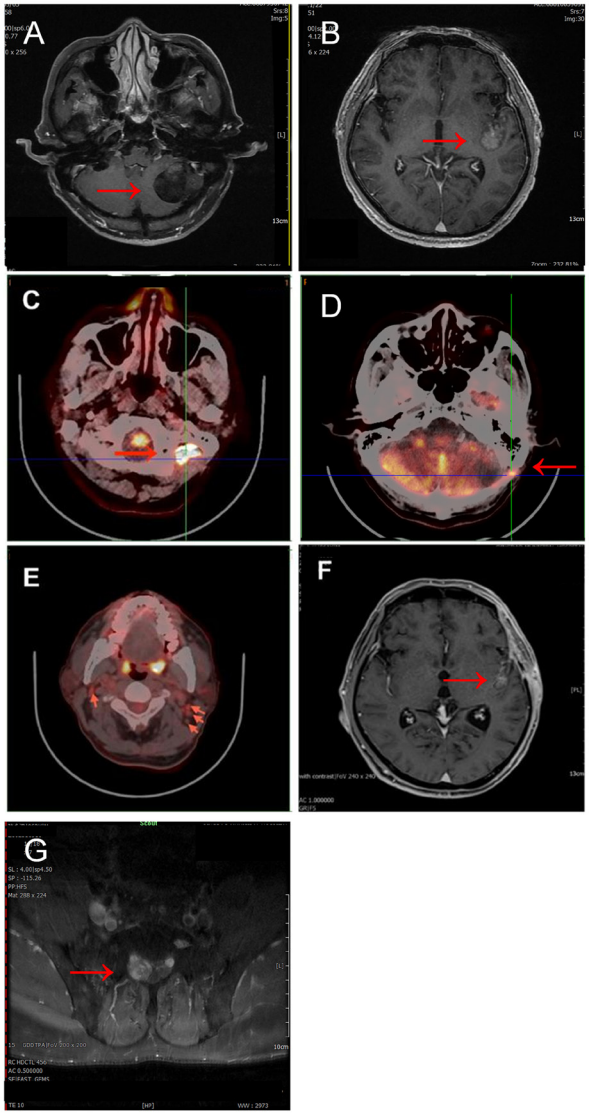

Figure 1. Preoperative and follow-up images. (A) MRI performed in 2022 showing a lesion in the left cerebellar hemisphere presenting as uneven moderate enhancement. (B) MRI in 2023 showing an irregular mass-like enhancement in the left lateral fissure. (C) PET-CT in 2024 showing a low-density area in the left cerebellar surgical site. (D) PET-CT in 2024 showing soft-tissue nodules on the periphery and below the surgical area. (E) PET-CT in 2024 showing multiple hypermetabolic lymph nodes in the bilateral neck. (F) MRI in 2024 showing abnormal enhancement in the left insular-sylvian cistern area. (G) MRI in 2024 showing nodular abnormal signal foci in the sacral canal at the S1-2 level. MRI, magnetic resonance imaging; PET-CT, positron emission tomography-computed tomography.

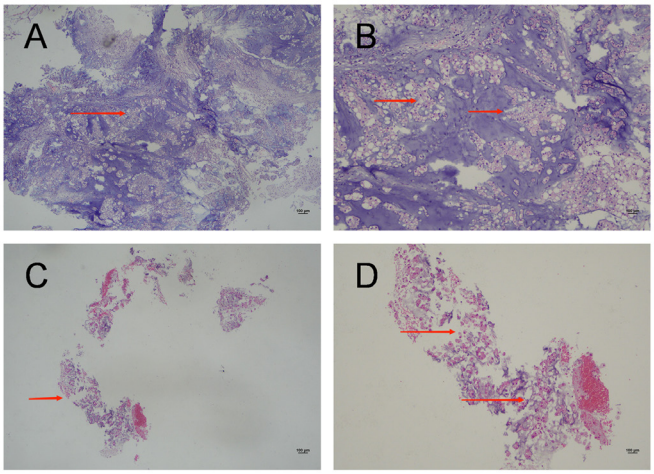

Figure 2. H&E images of two tumors. (A) An H&E image from 2022. Magnification, x4. Under low magnification, the tissue appears fragmented, with the tumor exhibiting a pattern of cords and nests within the blue myxoid matrix (arrow). (B) An H&E image from 2022. Magnification, x10. Under medium magnification, the tumor is composed of cords of epithelioid cells with vacuolated cytoplasm and collagen fibers within a basophilic stroma (arrows). (C) An H&E image from 2023. Magnification, x4. Under low magnification, the tissue appears fragmented and is accompanied by a small amount of blue-stained mucus (arrow). (D) A 2023 H&E image. Magnification, x10. Under medium magnification, the tumor is composed of cords and isolated epithelioid cells, which exhibit intracytoplasmic vacuoles within a myxoid matrix (arrows). H&E, haematoxylin and eosin.

During embryonic development, the upper end of the notochord is situated in the sphenoid and occipital bones at the base of the skull, while the lower end is located in the sacrum. Consequently, chordomas typically arise in the skull base or sacrum. The annual incidence rate of chordoma is ~0.8 per million individuals, accounting for ~1% of all bone tumors. Chordoma can manifest at any age; however, the majority of patients are diagnosed between the ages of 40 and 50 years, with <5% of cases occurring in individuals <20 years (1,7).

Clinical manifestations primarily depend on the location and extent of the lesions. Intracranial chordomas typically result in headaches or facial numbness due to the proximity of the tumor to cranial nerves, whereas sacrococcygeal chordomas lead to lumbosacral pain or bowel dysfunction as a consequence of compression of the sacral nerve roots (7).

Meningioma is a type of tumor that arises from the meninges, the protective membranes surrounding the brain and spinal cord. Chordoid meningiomas account for 0.5-1% of all meningiomas and are more commonly found in young female patients (8). These tumors are typically located in the supratentorial region or at the skull base, where they invade surrounding tissues, leading to associated symptoms such as headaches, vomiting and visual disturbances (3).

The clinical symptoms of chordoma and chordoid meningioma can often present similarly. The current patient presented at the hospital with complaints of dizziness, headaches and numbness in the right hand. There were no distinguishing symptoms to differentiate between the two tumors. While chordoma is known for its propensity to recur, meningioma typically does not exhibit this tendency. The recurrence of the tumor within <2 years aligns with the biological behavior of chordoma, prompting re-evaluation and revision of the initial pathology report.

Chordoma commonly originates from the sphenoid-occipital symphysis region and primarily grows in the midline area, typically involving the midline structures in the slope region. There is marked bone destruction at the skull base, particularly in areas such as the saddle dorsal and slope, and the tumor can extend into the adjacent basal cistern. Chordoma typically presents as a destructive lobulated mass on CT, which invades adjacent tissues and is associated with lytic bone destruction and soft-tissue expansion (9). MRI, with its high soft-tissue resolution, accurately depicts the location of the tumor, tissue structure and surrounding structures that it invades. T1-weighted imaging

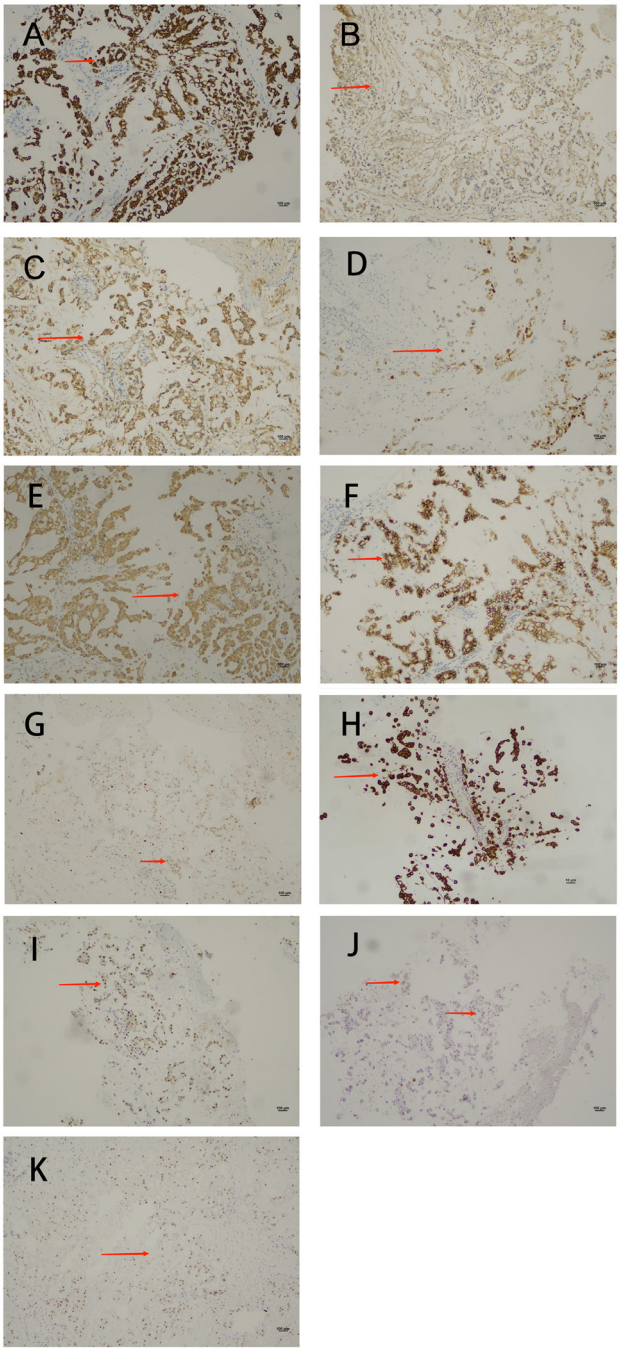

Figure 3. Immunohistochemistry images of tumors obtained from the first surgery. Arrows indicate positive staining. Magnification, x10. (A) A CK-positive image. (B) A vimentin-positive image. (C) An epithelial membrane antigen-positive image. (D) A synaptophysin-positive image. (E) An E-cadherin-positive image. (F) A CK8/18-positive image. (G) An image showing a Ki-67 proliferation index of 3%. (H-K) Immunohistochemistry images of tumors obtained from the second surgery. Arrows indicate positive staining. Magnification, x10. (H) A CK-positive image. (I) A Brachyury-positive cells. (J) A S100 weakly positive cells. (K) An immunohistochemistry image of the repeated analysis performed in 2023 for sections initially obtained in 2022, showing Brachyury-positive cells.

(T1WI) indicates low signal lesions, while T2-weighted imaging (T2WI) shows high signal lesions accompanied by low signal septations, resulting in a honeycomb-like pattern of uneven enhancement (9-11).

Chordoid meningioma in general is located in the supratentorial region and typically exhibits aggressive behavior on imaging, often invading surrounding bone while maintaining an intact capsule. Involvement of the brain parenchyma is rare (3). A CT scan typically reveals isodensity, while MRI often shows low signal using T1WI and high signal using T2WI. Some lesions may exhibit mixed signals with long T1 and long T2 characteristics, along with marked enhancement following contrast administration (11). Caudal meningeal signs may be present, and restricted diffusion on DWI is not limited (12).

The lesion in the present case was located adjacent to the skull base area of the posterior cranial fossa; however, there was no evident bone destruction in the adjacent skull, nor were there any signs of bleeding, necrosis, irregular calcification or other abnormalities within the lesion itself. The DWI signal of the lesion was not elevated, indicating that it was not prominently visible on imaging. There was no clear evidence of restricted diffusion, which suggests that the imaging findings did not align with typical clinical presentations of chordomas. The lesion in the present case presented as a hemicystic, low-density round mass on the plain CT scan. MRI signal characteristics revealed that T1WI predominantly exhibited low signal intensity, while T2WI demonstrated slightly elevated and uneven signal intensity, with additional patches of slightly low signal observed internally. The T2-fluid attenuated inversion recovery image displayed heterogeneous high signal intensity. Notably, most lesions on the enhanced scan did not exhibit enhancement, although an eccentric marginal area of pronounced heterogeneous enhancement was evident. These imaging characteristics are not consistent with typical clinical presentations of meningiomas. Therefore, this discrepancy contributed to the misdiagnosis.

The initial diagnosed lesion in the present case was situated in the left cerebellar hemisphere. The location of its onset is not a typical site for meningiomas in adults. Furthermore, the lesion did not exhibit the general characteristics associated with intracranial and extracerebral tumors on imaging. These characteristics include, but are not limited to, the white matter collapse sign, the meningeal tail sign, adjacent subarachnoid space widening and cerebrospinal fluid clefts (12). Additionally, the remaining lesions did not show a close relationship with the dura mater or the skull.

According to the 5th edition of the WHO classification of bone and soft-tissue tumors, chordoma is categorized into three types: Classic type, dedifferentiated type and poorly differentiated type (7). The pathology of classic chordoma is characterized by a fine fibrovascular connective tissue stroma, which contains trabecular and nest-like epithelioid cells within the lobules. The cell sizes vary, and the cells include multinucleated, stellate and vacuolated cells with abundant and intensely eosinophilic cytoplasm. The background features an abundant extracellular myxoid matrix, and necrosis is often observed, while mitotic figures are uncommon. Classic chordoma may exhibit both chordoma and chondroid features, previously referred to as chondroid chordoma; the 5th edition of the WHO classification of bone and soft tissue tumors includes chondroid chordoma under classic chordoma (4).

Dedifferentiated chordoma is a biphasic tumor characterized by the presence of two distinct components: A classic chordoma component and a high-grade sarcoma component. The high-grade sarcoma component usually manifests as either

Table I. Summary table of patient presentation.

Date	Patient presentation
March, 2022	The patient presented to the hospital with complaints of headaches and dizziness. MRI revealed a space-occupying lesion in the left cerebellar hemisphere. A resection of the skull base lesion was subsequently performed. The pathological diagnosis was chordoid meningioma. Postoperative radiotherapy was then administered.
November, 2023	The patient presented to the hospital with facial numbness on the right side. MRI revealed an intracranial space-occupying lesion. The patient subsequently underwent resection of the skull base lesion, and the pathological diagnosis was chordoma.
December, 2023	The patient underwent local radiotherapy for intracranial lesions and the sacral vertebra following surgery, with the treatment's efficacy assessed as a partial response.
March, 2024	Positron emission tomography-computed tomography scans revealed a space-occupying lesion in the left cerebellar surgical site. Given the potential for tumor recurrence, palliative radiotherapy was administered to the area of recurrence, and the efficacy of this treatment was evaluated as progressive disease.
November, 2024	The patient experienced episodes of paroxysmal dizziness, and MRI enhancement revealed nodular abnormal signal foci within the sacral canal. The possibility of chordoma recurrence was considered, and targeted therapy with imatinib was administered.

MRI, magnetic resonance imaging.

high-grade undifferentiated spindle cell sarcoma or high-grade osteosarcoma. Tumor cells may display binucleation or multinucleation, and mitotic figures are often observable (4). The 5th edition of the WHO classification of bone and soft-tissue tumors categorizes poorly differentiated chordoma as a new subtype. This subtype has a low incidence rate, primarily occurring in children and young adults, and is commonly located at the skull base. Pathological features include a solid growth pattern and notable cellular atypia, which is characterized by the loss of integrase interactor 1 (INI1) expression (4).

The pathology of chordoid meningioma is characterized by tumor cells arranged in nests or trabecular patterns, featuring eosinophilic cytoplasm and intracellular vacuoles. The stroma has a myxoid appearance, and mitotic figures are rare. Classic areas of meningioma are frequently observed in the surrounding tissue, displaying a swirling, bundle-like pattern, while pure chord meningioma is uncommon (13).

When the chordoid areas predominate or when tumors exhibit chondroid metaplasia, accurate morphological diagnosis can be problematic as the differential diagnosis broadens to include chordoid glioma, skeletal/extraskeletal myxoid chondrosarcomas, chondrosarcomas and enchondromas. The immunohistochemical evaluation is particularly effective for differentiating these tumors (13) (Table II).

Chordomas and chordoid meningiomas exhibit marked histological similarities. In the present study, the pathology report from the first surgery revealed cord-like epithelioid cells, myxoid stroma and meningioma-like regions in certain adjacent areas. However, due to the limited number of gross specimens available, there were insufficient regions for accurate identification, leading to a misdiagnosis.

Chordoma expresses CK8, CK18 and CK19, but does not express CK7 and CK20. Both EMA and S100 protein are positive in chordomas (14,15). Brachyury, a transcription factor encoded by the T gene located on chromosome 6q27, serves a crucial role in embryonic notochord development and is considered a key driver of chordoma (16). When utilized for the diagnosis of chordoma, Brachyury demonstrates high specificity and sensitivity, with a positive rate reaching as high as 99%. In poorly differentiated chordoma, tumor cells are positive for broad-spectrum CK and Brachyury, whereas in dedifferentiated chordoma, expression of all markers may be negative (17,18). Chordoid meningioma typically exhibits positivity for vimentin, EMA and PR, while S100, CK and GFAP are generally negative. Sangoi *et al* (13) reported a higher positive rate of D2-40 in chordoid meningioma, highlighting its diagnostic importance.

Chordoma and chordoid meningioma share numerous immunohistochemical similarities. Brachyury, an antibody that has received focus in recent years, is infrequently utilized for diagnoses other than chordoma. Therefore, numerous pathologists may not fully recognize its importance. This lack of awareness is also the reason why Brachyury was not included in the initial pathology assessment for the present patient.

In addition to Brachyury, mutations in genes such as cyclin-dependent kinase inhibitor 2A (CDKN2A), PTEN and INI1 have also been identified in chordoma (19-21). INI1 is a tumor suppressor protein that serves as a component of the SWItch/Sucrose Non-Fermentable (SWI/SNF) complex, which regulates gene expression through the remodeling of chromatin structure. Deletion or mutation of the INI1 gene results in decreased protein expression, thereby impairing the normal function of the SWI/SNF complex. This impairment may subsequently lead to abnormal cell proliferation and tumor formation (22). A recent study demonstrated that the immunohistochemical loss of INI1 protein in poorly differentiated chordoma primarily results from

Table II. Pathological distinctions of tumors of the central nervous system with marked histological overlap.

Tumor	Site	Tumor structure	Tumor cells	Tumor stroma	Positive immunohistochemistry results	Genetics	(Refs.)
Chordoma	Skull base or sacrum	Lobulated structure	The cell sizes vary, and the cells include multinucleated, stellate and vacuolated cells with abundant and intensely eosinophilic cytoplasm	Extracellular myxoid matrix	CK8, CK18, CK19, EMA, S100, Brachyury	Mutations in Brachyury, CDKN2A, PTEN, SMARCB1	(16,36)
Chordoid meningiomas	Supratentorial region or at the skull base	Tumor cells arranged in cords or nests	The tumor cells arranged in nests or trabecular patterns, featuring eosinophilic cytoplasm and intracellular vacuoles	Myxoid matrix	Vimentin, EMA, PR	Deletion of 1p, 2q/NF2 and CDKN2A/B	(2,8)
Chordoid glioma	Third ventricle	Lobulated structure, with tumor cells arranged in clusters and cords	The tumor cell displays characteristics of epithelial cells, including abundant, deeply stained cytoplasm and oval or round nuclei	Myxoid or vacuolated matrix	GFAP, TTF-1	p.D463H mutation in the PRKCA gene	(37,38)
Skeletal/ extraskeletal myxoid chondrosarcomas	Deep soft tissues of the proximal limbs, particularly in the lower limbs	Lobulated structure, with tumor cells arranged in cords, small clusters or grids	The nuclei of the tumor cells are small and exhibit deep staining, while the cytoplasm is eosinophilic and partially vacuolated	Myxoid or myxochondral matrix	Vimentin, S100, EMA, CD99, SOX9	>75% of cases contain the t(9;22)(q22-31;q11-12) chromosome translocation. The NR4A3 fusion gene can be detected in >90% of cases	(39,40)
Chondrosarcomas	Pelvis and proximal femur	Lobulated structure	Tumor cells are dense at the edges of the lobules and sparse in the center. Tumor cells are observed to be round, triangular or star-shaped and are located within cartilage cavity	Cartilage matrix	S100, SOX-10	~50% of the tumors presented heterozygous missense mutations in IDH1 R132 and IDH2 R172	(41,42)
Enchondroma	Metaphyseal region of the long bones	Lobulated hyaline cartilage nodules	The nuclei of tumor cells are small, round and darkly stained, while the cytoplasm is abundant in vacuoles	Cartilage matrix	Lacks specific immunohistochemical features	Mutations in the IDH1/2 genes	(42)

CK, cytokeratin; CDKN, cyclin-dependent kinase inhibitor; IDH, isocitrate dehydrogenase 1; EMA, epithelial membrane antigen; GFAP, glial fibrillary acidic protein; PR, progesterone receptor; SMARCB1, SWI/SNF related BAF chromatin remodeling complex subunit B1; NF2, NF2, moesin-ezrin-radixin like tumor suppressor; NR4A3, nuclear receptor subfamily 4 group A member 3; TTF-1, transcription termination factor 1.

a homozygous deletion of the 22q11 locus (4). The loss of INI1 protein may provide a rationale for assessing the efficacy of novel targeted therapies, such as enhancer of zeste homolog 2 (EZH2) inhibitors. EZH2 serves as the catalytic subunit of the histone methyltransferase polycomb repressive complex 2, and its upregulation has been linked to the promotion of carcinogenesis. EZH2 inhibitors have demonstrated the ability to induce tumor regression and enhance radiosensitivity in SWI/SNF-related BAF chromatin remodeling complex subunit B1/INI1-deficient tumor models (23). INI1 immunohistochemistry was performed on the two surgical specimens of the patient, both of which demonstrated weak positivity in a few scattered cells (data not shown). Horbinski *et al* (24) reported that deletions of 1p36 and 9p in chordoma were linked to decreased overall survival (OS). Furthermore, Wei *et al* (25) demonstrated that reduced H3K27me3 epigenetic modification in chordoma was associated with a poor prognosis. H3K27me3 is a main epigenetic modification, primarily mediated by EZH2, the catalytic subunit of the histone methyltransferase PRC2 complex. H3K27me3 is essential for the regulation of gene expression and is frequently associated with gene silencing (26).

A previous study identified microRNA (miR)-1, miR-31 and miR-148a as promising prognostic and therapeutic markers for chordoma (27). Additionally, Brachyury vaccines and molecular targeted therapies have been explored as potential treatment options for this condition (28). The preferred treatment method for chordoma is surgical intervention; however, the proximity of vascular and nerve structures to the tumor often hinders complete resection, resulting in a high risk of recurrence. Chordomas exhibit a poor response to conventional radiotherapy and chemotherapy, which renders these modalities ineffective as standard treatment options (29). A study involving 357 patients with chordoma performed in the United States revealed OS rates of 80.5, 68.4 and 39.2% at 3, 5 and 10 years, respectively. Additionally, the disease-specific survival rates at these intervals were 89.0, 80.9 and 60.1%, respectively. It was observed that when patients were >60 years old or received non-surgical treatment due to metastasis, the OS rate declined (30).

Daoud *et al* (31) identified that common copy number variations in chordoid meningioma included a deletion of 1p, whereas deletions of 22q/NF2, moesin-ezrin-radixin-like tumor suppressor and CDKN2A/B were molecular alterations associated with tumor recurrence and progression. In the present study, the patient refused to undergo molecular testing, and the small size of the tumor tissue rendered pathological testing unfeasible. It is essential for physicians to collect additional specimens during surgery for molecular testing, thereby offering patients a broader range of treatment options.

The preferred treatment for chordoid meningioma is surgical intervention, and the grade of meningioma resection, as categorized by the Simpson grading system, serves as a prognostic factor. For patients in whom a Simpson grade II resection cannot be achieved, postoperative radiotherapy is necessary (32). Ren *et al* (33) indicated that the progression-free survival (PFS) of patients with chordoid meningioma was improved compared with that of patients with non-chordoid WHO Grade 2 meningioma, yet worse than that of patients with WHO Grade 1 meningioma. Additionally, the OS of chordoid meningioma was superior to that of non-chordoid WHO Grade 2 meningioma. Furthermore, recurrence status and adjuvant radiotherapy were identified as independent prognostic factors for both PFS and OS (33).

Although the misdiagnosis did not affect the surgical method in the present study, it influenced the treatment approach and prognosis. If the initial diagnosis had been accurate and radiotherapy for chordoma had been administered promptly, the prognosis of the patient would likely have been more favorable than it currently is. The lesion was situated in the cerebellum, and the primary approach was resection of the skull base lesion. The planning target volume (PTV) for radiotherapy following the first operation was 5,040 cGy/180 cGy/28 fractions, while the PTV for radiotherapy after the second operation was 4,000 cGy/200 cGy/20 fractions for intracranial lesion, 7,000 cGy/200 cGy/35 fractions for lumbosacral. If chordoma was confirmed during the first operation, an appropriate radiotherapy could have been utilized to decrease the recurrence rate.

Pathology was the primary reason for the misdiagnosis and subsequent mistreatment of the present patient. Initially, the workflow of the pathology was flawed; the report was issued by a single pathologist without review by a specialist or general discussion. Due to a lack of experience in diagnosing chordoma in the brain, the pathologist mistakenly classified the chord-like cells as chordoid meningiomas, overlooking the potential diagnosis of chordoma. Consequently, immunohistochemical staining for vimentin, EMA, GFAP and S100, along with a negative result for CD34, supported the erroneous conclusion of chordoid meningioma. Unaware of the distinctions between chordoma and chordoid meningioma, the pathologist did not perform the Brachyury test. Furthermore, no imaging studies were performed to assess the positional relationship between the tumor and the meninges. Following recurrence, the original pathologist reviewed the initial pathology and, upon consultation with a specialist, raised the possibility of chordoma and recommended the Brachyury test for confirmation. The positive result validated the diagnosis of chordoma and highlighted the initial misdiagnosis. Rekhi and Karmarkar (34) demonstrated that immunohistochemistry is crucial for differentiating between these two entities, recommending the use of CK, GFAP, vimentin, EMA, S100, PR, D2-40 and Brachyury. Therefore, caution is advised when certain immunohistochemical markers are absent, and it is prudent to seek consultation from a more experienced pathologist if necessary.

From a clinical perspective, the current patient presented with a lack of specific clinical symptoms, and the site of onset was not typical for a chordoma. Consequently, after receiving a pathological diagnosis of meningioma, the clinician did not engage in further communication with the pathologist.

In terms of imaging, the two preoperative MR diagnoses indicated only intracranial space occupation without specifying the tumor type or the potential for benign or malignant characteristics. Following the second recurrence of the tumor and subsequent pathological diagnosis, PET-CT revealed multiple metastases throughout the body and suggested a diagnosis of chordoma. The misdiagnosis prompted the

development of a novel pathology process: All reports must now be diagnosed by two pathologists. Additionally, in challenging cases, it is essential to communicate with imaging specialists and clinicians, and to conduct a multidisciplinary team meeting when necessary. Brachyury has been incorporated into the meningioma immunohistochemistry panel to aid in the differentiation between meningiomas and chordomas.

There are limitations to the present case report. Molecular/genetic testing was not performed in the current case report and limited tissue was available for diagnosis. While double staining for S100 and Brachyury could assist in identifying similar cases, both antibodies used in Qingdao Municipal Hospital stain the nucleus. Currently, technology does not allow for the double staining of antibodies that both target the nucleus. Consequently, this method was not employed to further verify the diagnosis.

To the best of our knowledge, the current case represents the first reported instance of such a misdiagnosis. Previous discussions have predominantly concentrated on the pathological differentiation between chordoma and chordoid glioma, with only one reported case of a chordoid meningioma being misdiagnosed as a chordoma (35). Therefore, the present case serves to enhance the understanding of chordoma and chordoid meningioma, ultimately improving diagnostic accuracy.

Acknowledgements

Not applicable.

Funding

No funding was received.

Availability of data and materials

The data generated in the present study may be requested from the corresponding author.

Authors' contributions

DL analyzed and interpreted the patient data, and contributed to writing the manuscript. CJ and MMZ performed the pathological examination. DL, MMZ and CJ confirm the authenticity of all the raw data. TW made substantial contributions to the acquisition and interpretation of all imaging data (MRI, PET-CT), critical analysis of radiological-pathological data and revision of the manuscript for important intellectual content regarding imaging findings. PZ provided analysis of clinical data. All authors read and approved the final version of the manuscript.

Ethics approval and consent to participate

Written informed patient consent was obtained. The present study was conducted with the approval of the Independent Ethics Committee of the Qingdao Municipal Hospital.

Patient consent for publication

Written informed consent was obtained from the patient for publication of the present case report.

Competing interests

The authors declare that they have no competing interests.

References

1. Karpathiou G, Dumollard JM, Dridi M, Dal Col P, Barral FG, Boutonnat J and Peoc'h M: Chordomas: A review with emphasis on their pathophysiology, pathology, molecular biology, and genetics. Pathol Res Pract 216: 153089, 2020.
2. Couce ME, Aker FV and Scheithauer BW: Chordoid meningioma: A clinicopathologic study of 42 cases. Am J Surg Pathol 24: 899-905, 2000.
3. Nambiar A, Pillai A, Parmar C and Panikar D: Intraventricular chordoid meningioma in a child: Fever of unknown origin, clinical course, and response to treatment. J Neurosurg Pediatr 10: 478-481, 2012.
4. Oakley GJ, Fuhrer K and Seethala RR: Brachyury, SOX-9, and podoplanin, new markers in the skull base chordoma vs chondrosarcoma differential: A tissue microarray-based comparative analysis. Mod Pathol 21: 1461-1469, 2008.
5. Medical Research Council: Nerve Injuries Committee. M.R.C. War Memorandum: Aids to the investigation of peripheral nerve injuries. Physical Therapy 23: 140, 1943.
6. Louis DN, Perry A, Wesseling P, Brat DJ, Cree IA, Figarella-Branger D, Hawkins C, Ng HK, Pfister SM, Reifenberger G, *et al*: The 2021 WHO classification of tumors of the central nervous system: A summary. Neuro Oncol 23: 1231-1251, 2021.
7. Choi JH and Ro JY: The 2020 WHO classification of tumors of soft tissue: Selected changes and new entities. Adv Anat Pathol 28: 44-58, 2021.
8. Lin JW, Ho JT, Lin YJ and Wu YT: Chordoid meningioma: A clinicopathologic study of 11 cases at a single institution. J Neurooncol 100: 465-473, 2010.
9. Santegoeds RGC, Temel Y, Beckervordersandforth JC, Van Overbeeke JJ and Hoeberigs CM: State-of-the-art imaging in human chordoma of the skull base. Curr Radiol Rep 6: 16, 2018.
10. Golden L, Pendharkar A, Fischbein NJc: Chapter 7 - Imaging Cranial Base Chordoma and Chondrosarcoma. In: Chordomas and Chondrosarcomas of the Skull Base and Spine. 2nd Edition. Elsevier Inc., pp67-78, 2018.
11. Farsad K, Kattapuram SV, Sacknoff R, Ono J and Nielsen GP: Sacral chordoma. Radiographics 29: 1525-1530, 2009.
12. Loken EK and Huang RY: Advanced meningioma imaging. Neurosurg Clin N Am 34: 335-345, 2023.
13. Sangoi AR, Dulai MS, Beck AH, Brat DJ and Vogel H: Distinguishing chordoid meningiomas from their histologic mimics: An immunohistochemical evaluation. Am J Surg Pathol 33: 669-681, 2009.
14. Lehtonen E, Stefanovic V and Saraga-Babic M: Changes in the expression of intermediate filaments and desmoplakins during development of human notochord. Differentiation 59: 43-49, 1995.
15. Folpe AL, Agoff SN, Willis J and Weiss SW: Parachordoma is immunohistochemically and cytogenetically distinct from axial chordoma and extraskeletal myxoid chondrosarcoma. Am J Surg Pathol 23: 1059-1067, 1999.
16. Vujovic S, Henderson S, Presneau N, Odell E, Jacques TS, Tirabosco R, Boshoff C and Flanagan AM: Brachyury, a crucial regulator of notochordal development, is a novel biomarker for chordomas. J Pathol 209: 157-165, 2006.
17. Dridi M, Boutonnat J, Dumollard JM, Peoc'h M and Karpathiou G: Patterns of brachyury expression in chordomas. Ann Diagn Pathol 53: 151760, 2021.
18. Miettinen M, Wang Z, Lasota J, Heery C, Schlom J and Palena C: Nuclear brachyury expression is consistent in chordoma, common in germ cell tumors and small cell carcinomas, and rare in other carcinomas and sarcomas: An immunohistochemical study of 5229 cases. Am J Surg Pathol 39: 1305-1312, 2015.
19. Scheil S, Brüderlein S, Liehr T, Starke H, Herms J, Schulte M and Möller P: Genome-wide analysis of sixteen chordomas by comparative genomic hybridization and cytogenetics of the first human chordoma cell line, U-CH1. Genes Chromosomes Cancer 32: 203-211, 2001.
20. Hallor KH, Staaf J, Jönsson G, Heidenblad M, Vult von Steyern F, Bauer HC, Ijszenga M, Hogendoorn PC, Mandahl N, Szuhai K and Mertens F: Frequent deletion of the CDKN2A locus in chordoma: Analysis of chromosomal imbalances using array comparative genomic hybridisation. Br J Cancer 98: 434-442, 2008.

21. Kuźniacka A, Mertens F, Strömbeck B, Wiegant J and Mandahl N: Combined binary ratio labeling fluorescence in situ hybridization analysis of chordoma. Cancer Genet Cytogenet 151: 178-181, 2004.
22. Roberts CW and Biegel JA: The role of SMARCB1/INI1 in development of rhabdoid tumor. Cancer Biol Ther 8: 412-416, 2009.
23. Kim KH and Roberts CWM: Targeting EZH2 in cancer. Nat Med 22: 128-134, 2016.
24. Horbinski C, Oakley GJ, Cieply K, Mantha GS, Nikiforova MN, Dacic S and Seethala RR: The prognostic value of Ki-67, p53, epidermal growth factor receptor, 1p36, 9p21, 10q23, and 17p13 in skull base chordomas. Arch Pathol Lab Med 134: 1170-1176, 2010.
25. Wei J, Wu J, Yin Z, Li X, Liu Y, Wang Y, Wang Z, Xu C and Fan L: Low expression of H3K27me3 is associated with poor prognosis in conventional chordoma. Front Oncol 12: 1048482, 2022.
26. Margueron R and Reinberg D: The polycomb complex PRC2 and its mark in life. Nature 469: 343-349, 2011.
27. Karele EN and Paze AN: Chordoma: To know means to recognize. Biochim Biophys Acta Rev Cancer 1877: 188796, 2022.
28. Heery CR, Palena C, McMahon S, Donahue RN, Lepone LM, Grenga I, Dirmeier U, Cordes L, Marté J, Dahut W, *et al*: Phase I study of a poxviral TRICOM-based vaccine directed against the transcription factor brachyury. Clin Cancer Res 23: 6833-6845, 2017.
29. Yurter A, Sciubba D, Gokaslan Z, Kaloostian PJJN: Spinal Chordomas: Current Medical and Surgical Management: JSM Neurosurgery and Spine, 2014.
30. Pan Y, Lu L, Chen J, Zhong Y and Dai Z: Analysis of prognostic factors for survival in patients with primary spinal chordoma using the SEER Registry from 1973 to 2014. J Orthop Surg Res 13: 76, 2018.
31. Daoud EV, Zhu K, Mickey B, Mohamed H, Wen M, Delorenzo M, Tran I, Serrano J, Hatanpaa KJ, Raisanen JM, *et al*: Epigenetic and genomic profiling of chordoid meningioma: Implications for clinical management. Acta Neuropathol Commun 10: 56, 2022.
32. Tahta A, Genc B, Cakir A and Sekerci Z: Chordoid meningioma: Report of 5 cases and review of the literature. Br J Neurosurg 37: 41-44, 2023.
33. Ren L, Hua L, Deng J, Cheng H, Wang D, Chen J, Xie Q, Wakimoto H and Gong Y: Favorable long-term outcomes of chordoid meningioma compared with the other WHO grade 2 meningioma subtypes. Neurosurgery 92: 745-755, 2023.
34. Rekhi B and Karmarkar S: Clinicocytopathological spectrum, including uncommon forms, of nine cases of chordomas with immunohistochemical results, including brachyury immunostaining: A single institutional experience. Cytopathology 30: 229-235, 2019.
35. Murali R and Ng T: Chordoid meningioma masquerading as chordoma. Pathology 36: 198-201, 2004.
36. Presneau N, Shalaby A, Ye H, Pillay N, Halai D, Idowu B, Tirabosco R, Whitwell D, Jacques TS, Kindblom LG, *et al*: Role of the transcription factor T (brachyury) in the pathogenesis of sporadic chordoma: A genetic and functional-based study. J Pathol 223: 327-335, 2011.
37. Goode B, Mondal G, Hyun M, *et al*: A recurrent kinase domain mutation in PRKCA defines chordoid glioma of the third ventricle. Nat Commuml 9: 810, 2018.
38. Reifenberger G, Weber T, Weber RG, Wolter M, Brandis A, Kuchelmeister K, Pilz P, Reusche E, Lichter P and Wiestler OD: Chordoid glioma of the third ventricle: Immunohistochemical and molecular genetic characterization of a novel tumor entity. Brain Pathol 9: 617-626, 1999.
39. Ogura K, Fujiwara T, Beppu Y, Chuman H, Yoshida A, Kawano H and Kawai A: Extraskeletal myxoid chondrosarcoma: A review of 23 patients treated at a single referral center with long-term follow-up. Arch Orthop Trauma Surg 132: 1379-1386, 2012.
40. Flucke U, Tops BBJ, Verdijk MAJ, van Cleef PJH, van Zwam PH, Slootweg PJ, Bovée JVMG, Riedl RG, Creytens DH, Suurmeijer AJH and Mentzel T: NR4A3 rearrangement reliably distinguishes between the clinicopathologically overlapping entities myoepithelial carcinoma of soft tissue and cellular extraskeletal myxoid chondrosarcoma. Virchows Archiv 460: 621-628, 2012.
41. Amary MF, Bacsi K, Maggiani F, Damato S, Halai D, Berisha F, Pollock R, O'Donnell P, Grigoriadis A, Diss T, *et al*: IDH1 and IDH2 mutations are frequent events in central chondrosarcoma and central and periosteal chondromas but not in other mesenchymal tumours. J Pathol 224: 334-343, 2011.
42. Pansuriya TC, van Eijk R, d'Adamo P, van Ruler MAJH, Kuijjer ML, Oosting J, Cleton-Jansen AM, van Oosterwijk JG, Verbeke SLJ, Meijer D, *et al*: Somatic mosaic IDH1 and IDH2 mutations are associated with enchondroma and spindle cell hemangioma in Ollier disease and Maffucci syndrome. Nat Genet 43: 1256-1261, 2011.